Parameterization Transition for Guided C^2 Surfaces of Low Degree

K. Karčiauskas and J. Peters

Abstract. By separating shape design from representation, the guided approach to surface construction [KP07] allows to routinely construct everywhere C^2 surfaces with (infinite) subdivision structure. This paper shows a *finite* guided C^2 surface construction of degree (6,6), albeit with many pieces, that preserves the good algebraic properties of the construction of kth order smooth surfaces of least degree in [Pet02], while avoiding geometric degeneration.

§1. Introduction

The paper describes the construction of a n-sided piecewise polynomial surface piece suitable for completing a C^2 tensor-product surface where n pairwise-joined primary surfaces join. For example, the piece fills an n-sided hole in a tensor-product spline surface (Fig. 11). The result is a surface of degree at most (6,6) with central patches joining at the extraordinary point of degree (4,4). This is good from an algebraic point of view and the shape is controlled by a local guide surface that can be used to express design intent or derived from existing constraints. Good shape and parametrization come at the cost of a large number of patches: if we include four guided subdivision steps, a cap with up to $55n$ polynomial pieces is generated. Nevertheless, we choose to present the construction here, since it illustrates a useful point of view about the interplay of parametrization, guide surfaces and sampling and since similar numbers of pieces have now become acceptable in the context of subdivision surfaces.

After reviewing the underlying techniques in Section 2 and the central (re-)parametrization σ of [Pet02] and ρ from [CC78, KP07] in Section 3, Section 4 explains the main contribution: the transition patchwork τ from ρ to σ. The capping construction is covered in Section 5. Due to page limitations, we refer to [KP07] for a broader survey of C^2 surface construction techniques.

Conference Title
Editors pp. 1–6.

ISBN 0-0-9728482-x-x

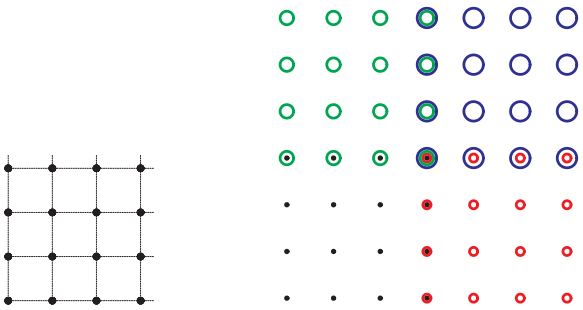

Fig. 1. (*left*) Sampled 4×4 corner block in Bézier form; (*right*) four corner bocks forming a Bézier patch of degree (6,6).

§2. Basic Techniques

The presentation assumes familiarity with the Bézier representation of polynomials and their derivatives along boundaries in terms of 'layers of coefficients', and concepts such as 'degree-raising' as explained in the textbooks [Far88, BP02].

Hermite sampling. A central component of the construction in [KP07] is a *Hermite sampling* operator h that is modified to an operator H that guarantees that rings join C^2. When applied to a map $f(s,t)$ defined over unit square, h creates a patch of degree (6,6) as follows (cf. Figure 1).

- At each corner, the partial derivatives of $f(s,t)$

$$\begin{array}{cccc} f & \partial_s f & \partial_s^2 f & \partial_s^3 f \\ \partial_t f & \partial_s \partial_t f & \partial_s^2 \partial_t f & \partial_s^3 \partial_t f \\ \partial_t^2 f & \partial_s \partial_t^2 f & \partial_s^2 \partial_t^2 f & \partial_s^3 \partial_t^2 f \\ \partial_t^3 f & \partial_s \partial_t^3 f & \partial_s^2 \partial_t^3 f & \partial_s^3 \partial_t^3 f \end{array}$$

  are sampled and converted into 4×4 corner block of Bézier coefficients of a polynomial piece of degree $(6,6)$ (Figure 1 *left*).
- At overlapping positions, the coefficients are averaged (Fig. 1, *right*).

Hermite sampling decouples the (high) degree of f (here the composition of a guide map with a parametrization of $\mathbb{R}^2$) from the degree of the resulting surface rings.

Guided Surface Rings. The tensor-product-spline compatible surface rings defined in [KP07] are shaped like a sprocket and therefore called *sprocket rings*. Each ring consists of $3n$ patches of degree (6,6) that join to yield a C^2 surface in the limit. The first sprocket ring can match second-order spline data at its outer boundary consisting of n spline curves. Such C^2 boundary data arise for example from the meeting of n tensor-product spline patches. The surface rings $\mathbf{x}^m$ are constructed by *sampling* the composition $\mathbf{g} \circ \lambda^m \rho$, where $\mathbf{g} : \mathbb{R}^2 \to \mathbb{R}^3$ is the guide and ρ a concentric

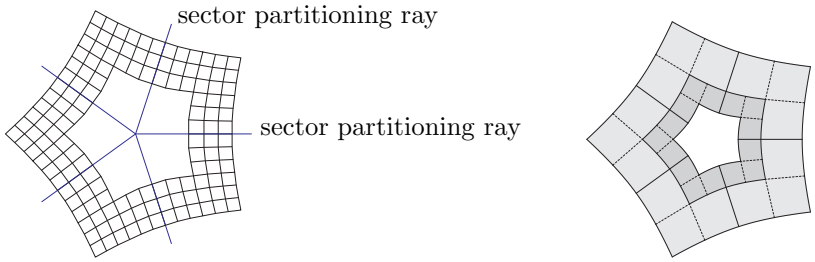

Fig. 2. (*left*) Bézier coefficients of one (bicubic) ring of ct-map for Catmull-Clark layout. (*right*) Two nested ct-maps.

tesselation map, short ct-map, i.e. a map whose scaled images $\lambda^m \rho$, $m = 0, 1, \ldots$ tesselate the neighborhood of the origin in a sequence of concentric annuli (see Figure 2, *right*). We align the *sector partitioning rays* (cf. Figure 2, *left*) of the tesselation map with the domain boundaries of the pieces of the guide surface and replace $\mathbf{g}$ by the lower-degree guide $\mathbf{q}$ after three steps.

Prolongation. When one ring is partitioned finer than its neighbor (see Figure 3 *middle*), there are two ways to make sure the connection is C^2 across T-junctions (Figure 3 *left*).

- *i-gluing* (Figure 3 *middle*): the innermost layers of the outer ring (with the coarser patch layout) determine the three outermost layers of Bézier coefficients of the inner ring;
- *e-gluing* (Figure 3 *right*): patches of the outer ring are subdivided (black lines) and their three innermost Bézier layers are adjusted to match the inner surface ring.

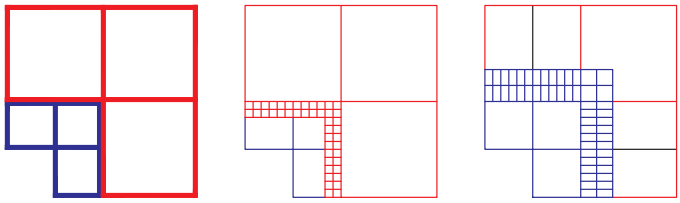

Fig. 3. Two options of gluing (*left*) the sampled patches: (*middle*) i-gluing by C^2 extension inwards; (*right*) e-gluing by C^2 extension outwards.

The sprocket rings in [KP07] are adjusted by i-gluing since i-gluing is consistent with the topology of ρ (the characteristic map of Catmull-Clark subdivision) and the iterated, λ-scaled nesting (Figure 3,*middle*) implies that i-glued and e-glued rings result in an almost identical curvature distribution. Here however, for the one-time transition to a finite parametri-

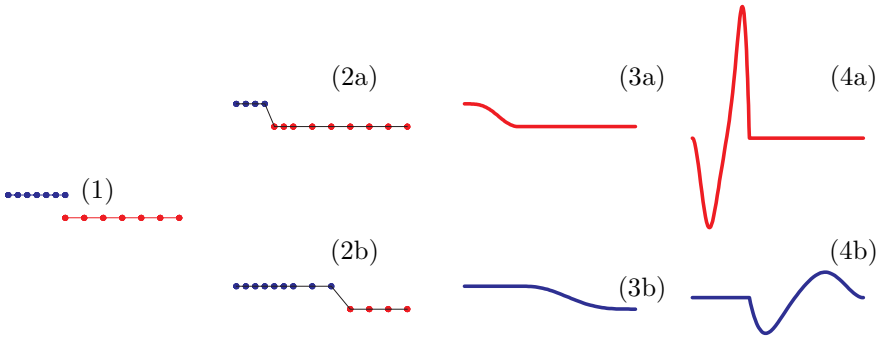

Fig. 4. (1) Spline control points of a univariate input to be C^2 blended; (2a) control net resulting from i-gluing; (3a) i-glued curve; (4a) curvature plots of the i-glued curve; (2b) control net resulting from e-gluing; (3b) e-glued curve; (4b) curvature plots of the e-glued curve.

zation as in Section 4, the more complex e-gluing pays off due to the more even distribution of curvature. This can be seen in the Gauss shading of the transition piece of the sector of the final surface in Figure 10. The effect is also illustrated, by univariate analogy, in Figure 4.

§3. Two planar parametrizations

The planar parametrization

$$\rho : \{1, \ldots, n\} \times [0..2]^2 \backslash [0..1]^2 \to \mathbb{R}^2$$

is the characteristic map of Catmull-Clark subdivision [CC78]. It is displayed in Figure 2, *left*. Since its λ-scaled copies tesselate a neighborhood of the origin, it is a concentric tesselation map, short ct-map, as defined in [KP07]. The second planar parametrization

$$\bar{\sigma} : \{1, \ldots, n\} \times [0..1]^2 \to \mathbb{R}^2,$$

defined originally in [Pet02], tesselates a regular n-gon and is determined, up to orientation and scaling, by rotating a template patch σ by $i \cos(\frac{2\pi}{n})$, $i \in \{1, \ldots, n\}$ about the origin. The x component of the bicubic Bézier control points σ_{jk} is symmetric

$$\begin{bmatrix} 0 & (1{+}c)(15{+}11\,c) & 6\,(1{+}c)(4{+}c) & 36{+}36\,c \\ (1{+}c)(15{+}11\,c) & 30{+}22\,c & 42{+}26\,c & 48{+}24\,c \\ 6\,(1{+}c)(4{+}c) & 42{+}26\,c & 48{+}16\,c & 60{+}12\,c \\ 36{+}36\,c & 48{+}24\,c & 60{+}12\,c & 72 \end{bmatrix},$$

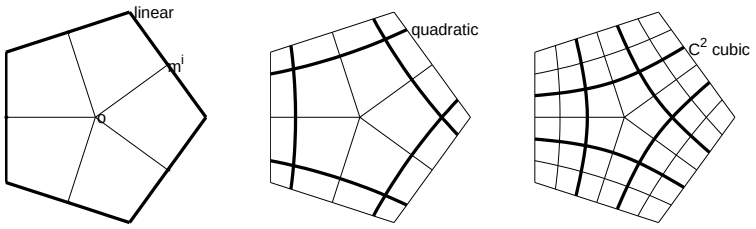

Fig. 5. The piecewise bicubic map $\bar{\sigma}$ (here shown rotated by π/n to show the symmetry with respect to the x-axis, $n = 5$), is defined by rings of linear, quadratic and cubic curves.

and the y component anti-symmetric (cf. Figure 5)

$$s \begin{bmatrix} 0 & 15{+}11\,c & 24{+}6\,c & 36 \\ -15{-}11\,c & 0 & 12{+}2\,c & 24 \\ -24{-}6\,c & -12{-}2\,c & 0 & 12 \\ -36 & -24 & -12 & 0 \end{bmatrix}, \qquad \begin{array}{l} c := \cos(2\pi/n), \\ s := \sin(2\pi/n) \end{array}.$$

The upper left entry corresponds to σ_{00} and the lower right to σ_{33}. The maps are best understood by their construction which consists of setting σ_{00} to be the origin and the remaining 15 control points of each piece to be the control points of symmetric families of curve segments in Bézier form.

a. The outermost curves are linear (Figure 5, *left*). Expressing these in Bézier form of degree 3 and subdividing at the midpoint creates 7 control points (Figure 5, *right*) per edge, i.e. the control points σ_{j3} and σ_{3j} for $j = 0, 1, 2, 3$.
b. The 7 control points of the second layer from each outer boundary represent a quadratic curve segment (Figure 5, *middle*), raised to degree 3 and subdivided at the midpoint. The first and the last Bézier control point of the ith quadratic segment are σ_{32} and σ_{23}. Subdividing at the midpoint and placing the middle control point of the quadratic on the diagonal from σ_{00} to σ_{33} uniquely determines the quadratic curve pieces. Degree-raising yields the control points σ_{j2} and σ_{2j}, $j = 0, 1, 2$.
c. The third layer of coefficients are the control points of a piecewise cubic curve (Figure 5, *right*). Two control points of each cubic are σ_{31}, σ_{21} respectively σ_{13} and σ_{12}. Two additional control points are pinned down by the C^2 join, and the shared final degree of freedom is used to place σ_{11} on the diagonal. This defines the remaining control points σ_{j1} and σ_{1j}, $j = 0, 1$.

We note that σ is, up to scaling and rotation, the *unique* symmetric C^2 finite tesselation map whose n rotated pieces form a regular n-gon. The

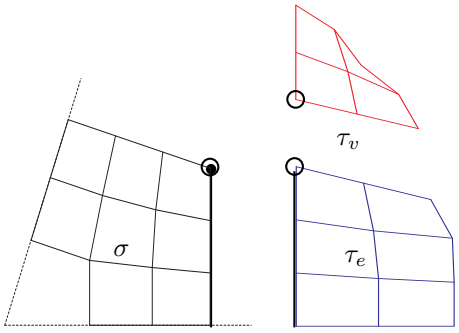

Fig. 6. Planar parametrization and extension for valence $n = 5$. The control nets are pulled apart for easier visualization of the three pieces. (*left*) One sector of σ; the origin is lower left. Note that all four boundaries are straight line segments. (*right*) Outward extensions of σ up to second order: τ_e across one side and (*right*, *top*) τ_v at the corner $\circ$ opposite the origin.

point of the construction, is that the first derivatives of the map across the n-gon are of low degree.

Lemma 1. *Let* $E := (1, [0..1])$ *denote the preimage under* σ *of a half-edge of the* n*-gon and* $deg_E(f)$ *the degree of map* f *restricted to* E*. Then for* $j = 0, 1, 2,$

$$deg_E(\partial^j \sigma) = j + 1.$$

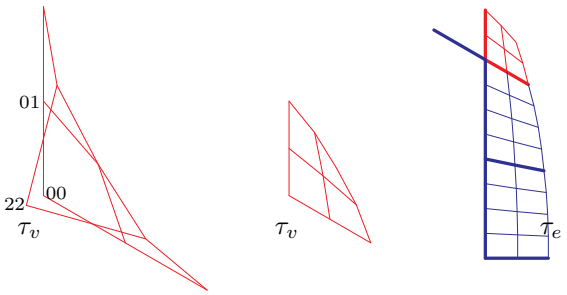

Fig. 7. Planar parametrization and extension for valence $n = 6$. (*left*) The outward extension at the corner has a self-overlapping control net in $\mathbb{R}^2$; (*middle*) outward corner extension when the domain of σ^k is scaled by $1/2$; (*right*) the combined effect of splitting and degree-raising.

While the algebraic properties resulting from the tesselation map σ are impressive (the partial derivatives of its composition with a map g of total degree d will be $\deg_E(\partial^j g \circ \sigma) = d + j$), Figure 6, *right*, *top*, gives a first

indication that the geometry of σ may lead to distortion near the n-gon vertex (marked $\circ$ in Figure 6) even though σ is regular at the vertex. Indeed, already for $n = 6$, the control polygon of the second-order Bézier net extension (jet) τ_v diagonally opposite the origin folds back on itself (Figure 7 *left*). Figure 7, *middle* and *right*, illustrate how splitting at 1/2 and degree-raising, while not changing the jet, result in a much more well-formed control net. We enforce such a neighboring parametrization of σ in the following construction of a transition patchwork τ from ρ to σ.

§4. Transition patchwork τ from ρ to σ in $\mathbb{R}^2$

For $n = 5, 6, \ldots, 10$, three steps of binary subdivision (and degree-raising to 4) yield a fair transition of the parametrization of the surrounding ct-map ρ to the innermost map σ (Figure 8). We ignore now higher valences

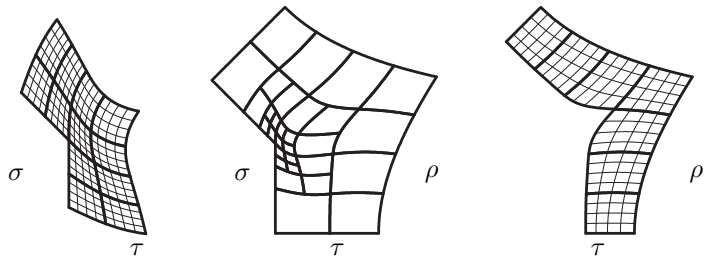

Fig. 8. (*middle*) Transition patchwork in $\mathbb{R}^2$ of degree (4,4) from ct-map ρ to the finite tesselation map σ for $n = 8$. (*left*) magnified view (scaled by 3) of the Bézier nets of the 12 biquartic patches at the polygonal internal corner of τ; (*right*) Bézier net of the seven biquartic patches adjacent to ρ.

and proceed as follows. Figure 8, *middle*, shows the overall structure of the transition map τ defined below.

(a) The finite tesselation map σ is twice locally refined by binary subdivision near the obtuse corner and the degree-raised to 4 result is e-glued to yield all inner three layers of Bézier coefficents of τ (Figure 9 *left*).

(b) The ct-map ρ is degree-raised to 4 and once refined (each patch split into four) and i-glued (Figure 8 *right*) yielding the outer three layers of Bézier coefficents of τ.

(c) C^2 gluing and symmetry constraints leave a transition map τ with 22 free parameters that are determined by minimizing $\mathcal{F}_4(\tau)$ the sum over all 21 pieces (Figure 9 *left*) where for the two coordinates (f_1, f_2), $\mathcal{F}_4(f_1, f_2) := \mathcal{F}_4(f_1) + \mathcal{F}_4(f_2)$ and

$$\mathcal{F}_4(f) := \int_0^1 \int_0^1 \sum_{i+j=4, i,j\geq 0} \binom{4}{i} (\partial_s^i f \partial_t^j f)^2.$$

(d) The three biquartics sharing the obtuse internal corner of σ are each split into four. This yields 30 pieces as shown in Figure 8, *middle* or Figure 9,*middle*. Figure 8, *left* shows a magnified view of this part.

We note that the construction, although not simple, depends only on the valence and for each valence be computed and stored once and for all.

§5. Capping patchwork in $\mathbb{R}^3$

With σ, τ and ρ at hand (computed once and for all), the construction in $\mathbb{R}^3$ for specific data is very simple. Working from the existing sprocket ring to the central point, we compute the surface by applying the operator H to a guide $\mathbf{q}$ of degree $d = 4$ composed with each of the parametrizations ρ, τ and σ.

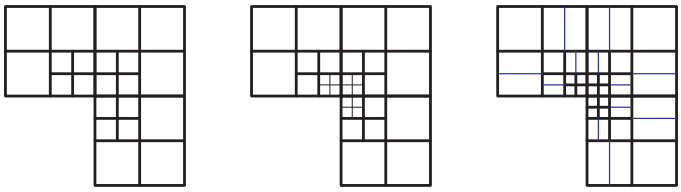

Fig. 9. (*left*), (*middle*) Two steps of building the transition patchwork τ in $\mathbb{R}^2$. (*right*) Final layout inherited by the degree (6,6) patchwork (in $\mathbb{R}^3$) after e-gluing.

- The T-junctions internal to $\mathbf{q}\circ\tau$ are removed and the rings are e-glued. The transition patchwork of one sector consists now of 42 bisextics as shown in Figure 9, *right*.
- The C^2 extension of $\mathbf{x}^{\mathbf{m}}$ (subdivided into four parts) replaces the three outermost layers of $h(\mathbf{q} \circ \tau)$ of degree (6,6), i.e. i-gluing is applied.

The resulting transition patchwork then smoothly joins the innermost cap reinterpreted as a bilineary trimmed piece of the guide $\mathbf{q}$.

Theorem 1. *Let $\beta : [0..1]^2 \to \mathbb{R}^2$ be a bilinear map with Bézier coefficients $\beta_{ij} := \sigma_{3i,3j}$, $i, j \in \{0, 1\}$. Then*

1) $\mathbf{q} \circ \beta$ and $\mathbf{q} \circ R\beta$ join G^2 (G^2 capping);

2) $\mathbf{q} \circ \beta$ and $H(\mathbf{q} \circ \tau)$ join G^2 (G^2 join to data);

3) deg$(\mathbf{q} \circ \beta) = (4, 4)$.

Proof: Since β and σ map the unit square to the same quadrilateral, $\beta([0..1]^2) = \sigma([0..1]^2)$, the point sets $\mathbf{q} \circ \beta([0..1]^2)$ and $\mathbf{q} \circ \sigma([0..1]^2)$ agree in $\mathbb{R}^3$ (the same piece of the C^2 guide surface is cut out). Therefore 1) holds because $\mathbf{q}\circ\sigma$ and $\mathbf{q}\circ R\sigma$ join G^2. By Lemma 1, $\deg_E(\partial^j \mathbf{q}\circ\sigma) = d+j$ for $j = 0, 1, 2$. (Recall that E is the preimage of of a half-edge of the n-gon). In particular, $\deg_E(\partial^j \mathbf{q} \circ \sigma) \leq 6$, and therefore $h(\mathbf{q} \circ \tau)$ reproduces

$\partial^j(\mathbf{q} \circ \sigma)$ along E. Therefore $\mathbf{q} \circ \sigma$ and $h(\mathbf{q} \circ \tau)$ join C^2 and, by the agreement of $\mathbf{q} \circ \sigma$ and $\mathbf{q} \circ \beta$ explained earlier, 2) holds. The cap $\mathbf{q} \circ \beta$ is of degree (4,4). □

Overall, the construction yields a sequence of surface rings of degree (6,6), followed by a G^2-capped by a cap of degree (4,4).

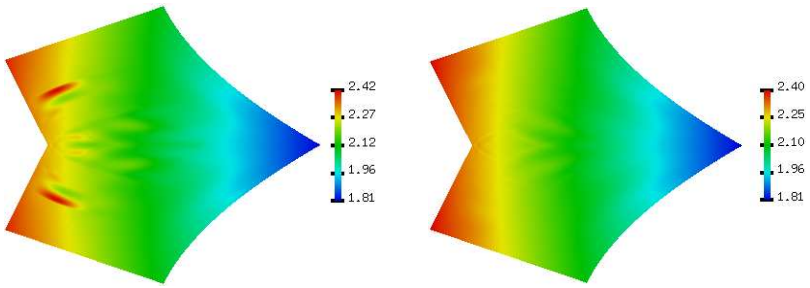

Fig. 10. Gauss shaded image of the transition $H(\mathbf{q} \circ \tau)$ of one sector as the result of i-gluing (*left*), respectively, of the proposed e-gluing (*right*). (cf. Fig. 3)

§6. Discussion

The construction results in a G^2 transition along an n-gon encircling the origin and a relative complex patch layout. Nevertheless, the local guide surface keeps the geometric complexity and variation under control. Figure 11, *right*, shows the Gaussian curvature-shaded surface overlaid with the Bézier nets (the dense mesh corresponds to the transition): comparing with Figure 11, *middle*, the complex transition is not apparent in the curvature (The mean curvature distribution is as clean as the displayed Gauss curvature). That is, the guided approach succeeds in separating the effects of parametrization from the design of the surface shape.

The construction is only made explicit for valences $n \leq 10$. While further cascading of of the transitional parameterization τ allows us to extend the quality of the construction to higher valence, for higher valence the patch layout should not be designed as a sprocket layout, but rather as a 'polar layout' [KP06].

Continuing to build on the guided approach, two alternative constructions have recently been discovered. The C^2 construction in [KP07a] consists of a single patch per sector, but is formally of degree (8,8). However, a degree (6,6) variant is visually, and even under close scrutiny of curvature, indistinguishable from the exact degree (8,8) surface. The C^2 construction in [KP07b] uses an unusual V-shaped layout to construct a surface with almost identical properties as the construction in this paper, but with fewer patches and no restriction on the valence.

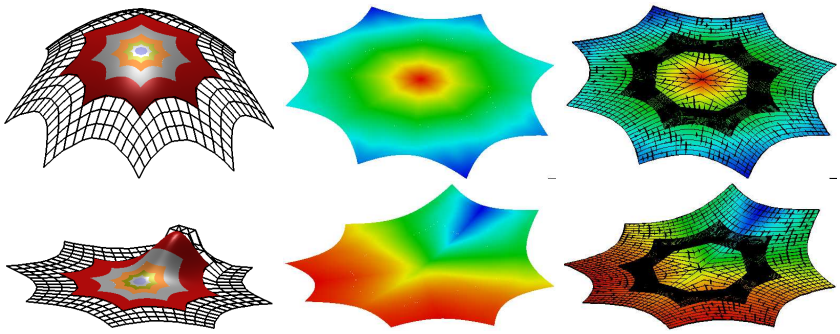

Fig. 11. (*top*) Convex cap (Gauss curvature is 1.5 to 2.8). (*bottom*) Cap for single bump. — (*left* column) shows the bicubic boundary data as Bézier net, guided surface rings $H(\mathbf{g} \circ \rho)$ with last ring $H(\mathbf{q} \circ \rho)$, transition $H(\mathbf{q} \circ \tau)$ and the final cap. (*middle* column) Gauss curvature and (*right*) Bézier net overlay.

References

BP02. Prautzsch Boehm and Paluzny. *Bézier and B-Spline Techniques.* Springer Verlag, 2002.

CC78. Catmull E., and J. Clark, Recursively Generated B-spline Surfaces on Arbitrary Topological Meshes. *Comp Aid Des*, 10(6): 350-355.1978

Far88. Farin, G. *Curves and Surfaces for Computer Aided Geometric Design — a Practical Guide.* Academic Press, Boston, MA, 1988.

KP06. Karčiauskas, K. and J. Peters, Surfaces with Polar Structure. *Computing* to appear.

KP07. Karčiauskas, K. and J. Peters. Concentric tesselation maps and guided surface rings. *Computer Aided Geometric Design*, 24(2), pages 99–111, 2007.

KP07a. Karčiauskas, K. and J. Peters, Guided C^2 Spline Surfaces, *Computer Aided Geometric Design*, in review.

KP07b. Karčiauskas, K. and J. Peters, Guided C^2 Spline Surfaces with V-shaped tessellation, submitted.

Pet02. Peters, J, C^2 free-form surfaces of degree (3,5). *Computer Aided Geometric Design*, 19(2):113–126, 2002.

Kęstutis Karčiauskas
Vilnius University
Vilnius, Lithuania
Kestutis.Karciauskas
@maf.vu.lt

Jörg Peters
University of Florida
Gainesville, FL, USA
jorg@cise.ufl.edu
http://www.cise.ufl.edu/∼jorg